TEMPERATURE AND TIME DEPENDENT FINITE-ELEMENT MODEL OF A THERMOELECTRIC COUPLE

Authors:
Paul G. Lau and Richard J. Buist

TE Technology, Inc.
1590 Keane Drive, Traverse City, Michigan 49686 USA

Abstract

The cooling performance of a thermoelectric (TE) couple is modeled from mathematical differential equations via finite-elements with the use of a digital computer. The finite-element model, which incorporates material property dependence on time and temperature, is presented. TE couple transient performance is investigated by applying an on-off current wave form to the model. Results from the model output are compared with experiment.

Introduction

A closed form solution of the complete differential equation for the temperature distribution in a thermoelectric (TE) pellet does not exist. This equation, of course, is further complicated when the transient of temperature with respect to time is included. Typically, simplifying assumptions are made to yield a closed form, albeit, inaccurate expression. However, the inaccuracies may be ameliorated by applying the closed-form expression to a number of finite elements which compose the TE couple.

Computational Model

The model was based on a one dimensional equation given by the following:[1]

$$SIT - \frac{1}{2}I^2R - K(T_H - T_C) = Q_c \qquad (1)$$

This equation, combined with energy conservation principles yields the following:

$$Q_p + Q_R + Q_K = \frac{m_j C_{pj}\left(T_j^{i+1} - T_j^i\right)}{t_{i+1} - t_i} \qquad (2)$$

where:

$$Q_p = IT_j^i\left(S_{j+1} - S_j\right) \qquad (3)$$

$$Q_R = \frac{1}{2}I^2\left(R_{j+1} + R_j\right) \qquad (4)$$

$$Q_K = K_{j+1}\left(T_{j+1}^i - T_j^i\right) + K_j\left(T_{j-1}^i - T_j^i\right) \qquad (5)$$

and:

Q_c = net heat pumping
I = current
S = Seebeck coefficient (temperature dependent)
R = resistance (temperature dependent)
K = thermal conductance (temperature dependent)
mC_p = mass times specific heat (assumed constant)
T = nodal temperature
t = time
i = time index
j = node index

Figure 1 depicts a pellet within a TE module showing the practical application of this equation.[2-4] However, in nodes (-1), (0), (40) and (41), the Joule heat and Peltier heat of the copper tab was assumed negligible compared with the pellet. Therefore, the model did not include those heats with respect to the copper tab. The pellet itself was divided into 40 elements. Each copper tab and ceramic, labeled on the top and bottom of the pellet was treated as a single element. The length-to-cross-sectional-area (L/A) ratio was calculated from the length of the finite-element divided by the cross-sectional area of the finite-element. The cross-sectional area of the ceramic finite-element was determined by using the overall cross-sectional area of the ceramic for the TE module divided by the total number of pellets. The cross-sectional area of the copper tab was calculated by taking one-half the overall cross-sectional area of the tab. However, the length of the tab finite-element was composed of the thickness of the tab plus the thickness of the solder. The effective thermal conductivity of the tab finite-element was derived from combining the actual thermal conductances of the copper tab and solder.

There were two cases for which experimental results could be readily obtained: 1) testing of a suspended TE module and 2) testing of a heat-sunk TE module. The test configurations for the suspended and heat sunk cases are shown in Figures 2 and 3, respectively. Referring back to Figure 1, the heat sink and interface medium did not apply to the suspended-module configuration. However, they were, of course, applied to the heat-sunk configuration. The model treated the heat sink as a node at constant temperature. The interface medium in the test was a thin film of water. It was treated in the model as an additional thermal conductance. The cross-sectional area of the interface was equivalent to the ceramic finite-element cross-sectional area. The thickness of the interface used in the model was 25.4 μm.

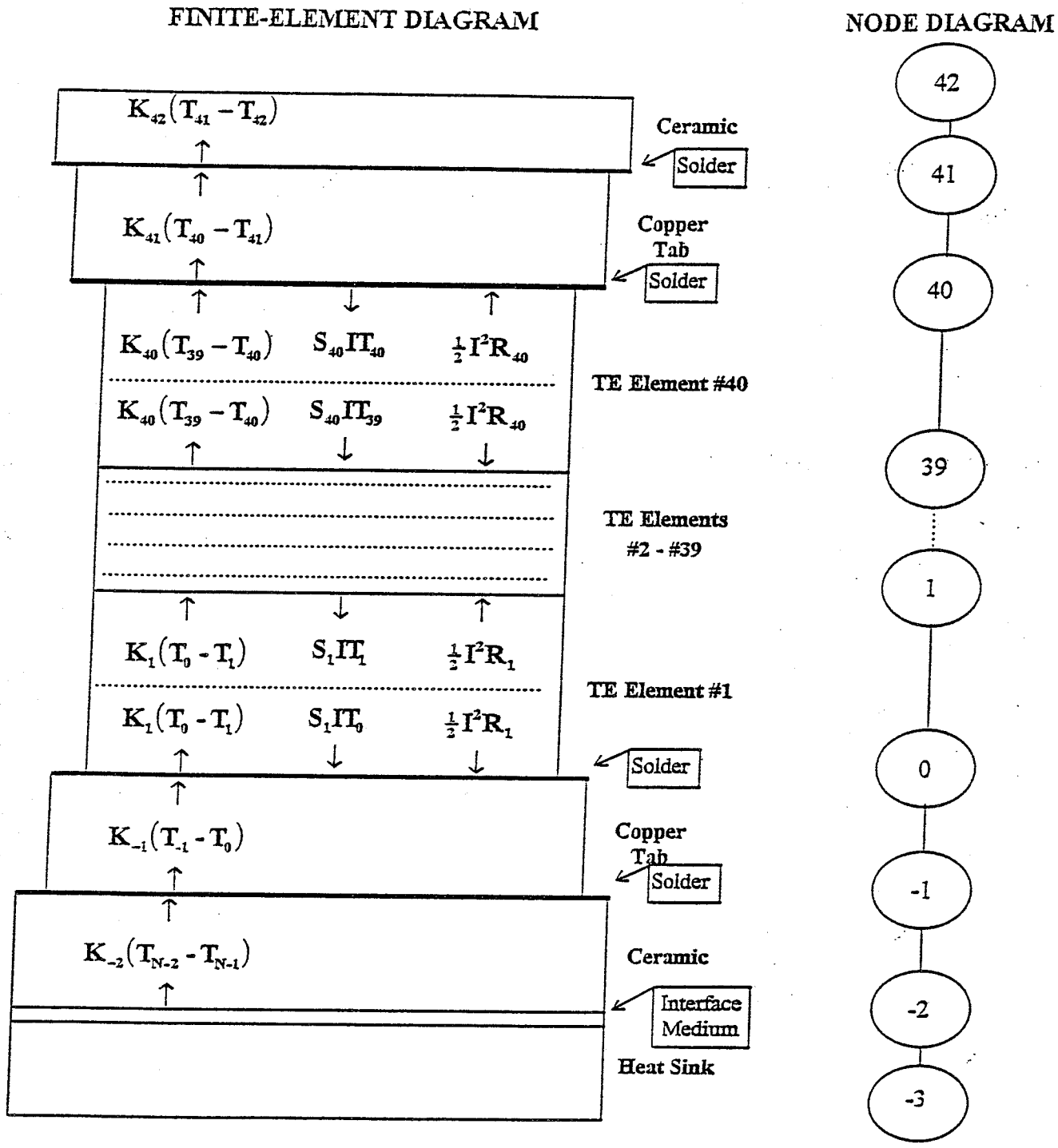

Fig. 1. Thermal Model Used for Transient Calculations

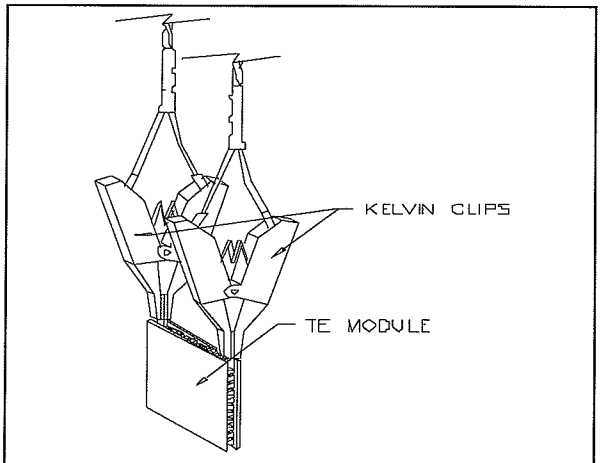

Fig. 2. Test Configuration for Suspended TE Module

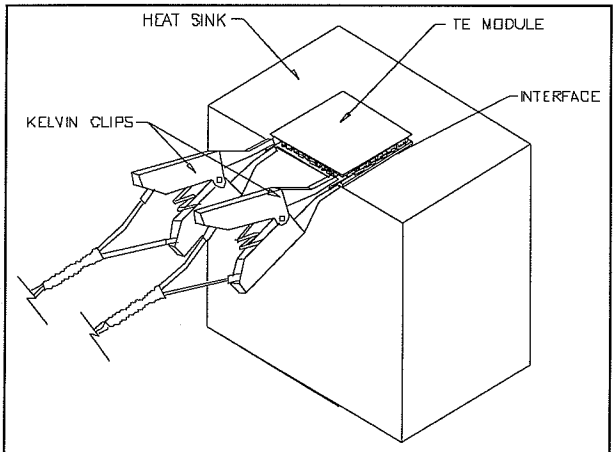

Fig. 3. Test Configuration for Heat Sink

Table 1
Tested Properties Of A 71 Couple Module
Pellet Dimensions=1.37mm x 1.37mm x 3.00mm

	Temp (°C)	Seebeck (μV/K)	Electrical Resistivity (μΩ•cm)	Thermal Conductivity (mW/cm/K)	Z (1000/K)
Suspended	22.99	203.6	1077.4	16.69	2.306
Suspended	23.02	203.7	1078.2	16.70	2.304
Suspended	23.02	203.6	1076.2	16.65	2.314
Suspended	23.06	203.8	1078.4	16.67	2.309
Suspended	23.10	203.6	1078.0	16.74	2.298
Suspended	23.12	203.8	1079.3	16.69	2.305
Heat Sunk	23.34	203.8	1080.8	16.76	2.292
Heat Sunk	23.35	203.7	1080.2	16.78	2.290
Heat Sunk	23.36	203.7	1081.9	16.86	2.274
Heat Sunk	23.39	203.8	1081.0	16.75	2.293
Heat Sunk	23.42	203.6	1079.8	16.79	2.287
Heat Sunk	23.44	203.7	1080.2	16.80	2.287

Table 2
Material Property Table

Material	Density g/cm^3	Specific Heat Capacity mJ/g/K	Thermal Conductivity mW/cm/K
TE Material	7.175	178.5	See Table 1
Ceramics	3.7	775	346
Copper Tab	8.91	385.2	4000
Solder	8.56	167	326.5
Water	1000	4.18	5.89

The material properties of the TE material were obtained by directly measuring the AC-resistance, the TE figure-of-merit and the pellet geometric dimensions. Proprietary algorithms in the test software provided predictions of the temperature-dependent properties for the Seebeck coefficient, thermal conductivity and electrical resistivity.[5] Table 1 shows the results of testing six times, for each configuration, the TE module's figure-of-merit, Z, and electrical resistivity, along with the projected Seebeck coefficient and thermal conductivity. The highlighted results for the two configurations were the bases for the temperature-dependent-TE properties used in the model. Other relevant material properties used in the model are given in Table 2. However, the properties listed in Table 2 were kept constant in the model. Also, all TE material properties were based on an N and P type average.[6]

Experimental Results

The suspended module configuration, shown in Figure 2, was tested with a current of 0.0885A, which was approximately 3% of Imax. This same test current was also used for testing the heat-sunk configuration. A small test current was used so that the temperature of the heat sink did not measurably change. The same TE module was used in all tests. All tests were performed using a model TS-205 computer automated test system supplied by TE Technology, Inc. Figure 4 shows the test results and model results for both test configurations.

Once a steady-state voltage had been established, the current was immediately set to zero and the decay voltage was measured. Figure 5 shows the test results and model results for both test configurations.

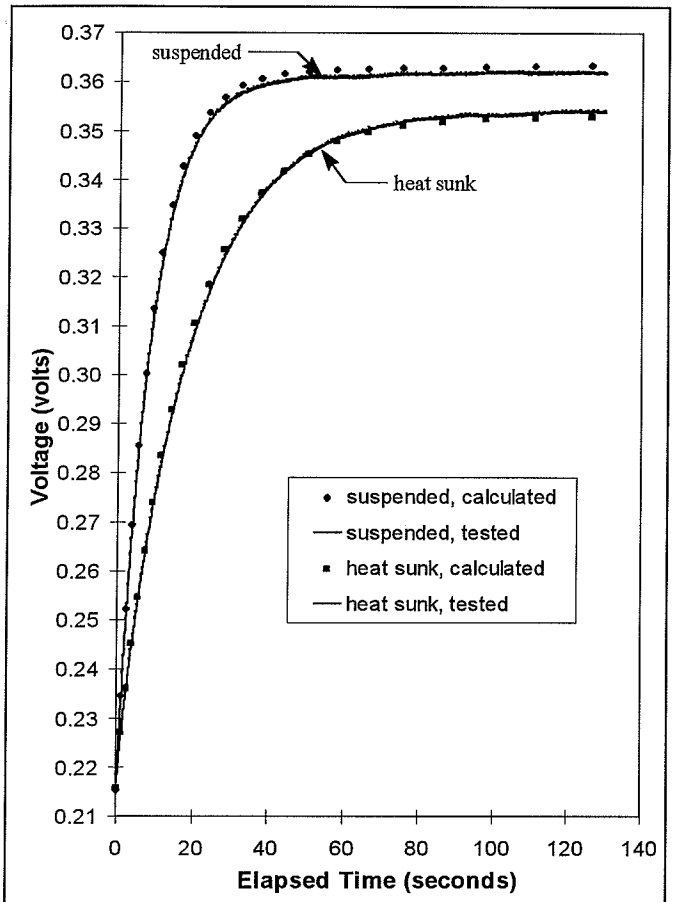

Fig. 4. Transient Response of Voltage. Power on. (Current = 0.0885 A)

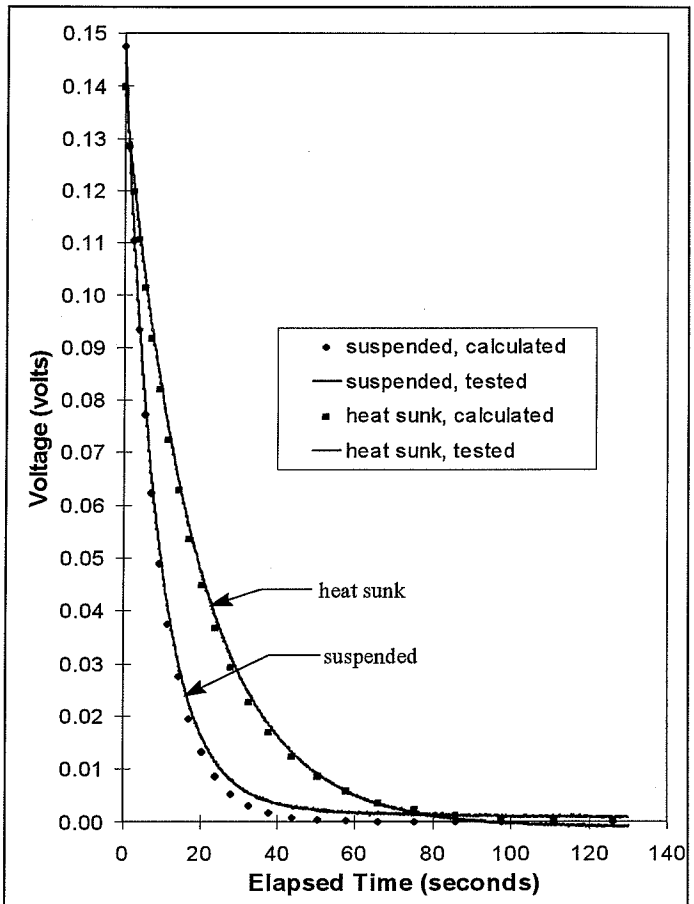

Fig. 5. Transient Response of Voltage. Power off. (Initially at steady state, Current = 0 A)

Figure 6 displays the model results of suspended module for temperature profiles at given time steps for the applied test current. Figure 7 shows how each nodal temperature varied with respect to time. Figures 8 and 9 are similar to Figures 6 and 7, respectively, except are for the power-off condition.

In Figures 4 and 5, the graphs show very little change in the voltage after about 30 seconds for the suspended module. This quasi-steady-state condition corresponds to the several parallel lines graphed in Figure 6. That is, as time increased beyond 30 seconds, the temperature-profile shape remained constant. As Figure 7 shows, the rate of increase in temperature of each node was constant after about 30 seconds. This corresponded to a constant temperature difference across the TE module which corresponded to a steady-state voltage.

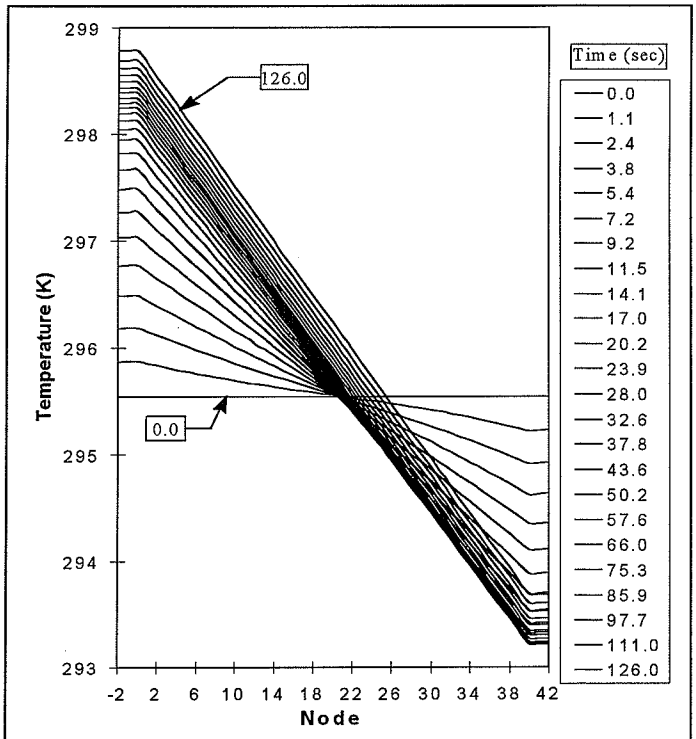

Fig. 6. Temperature Profiles for Suspended Module. Power on. (Current = 0.0885 A)

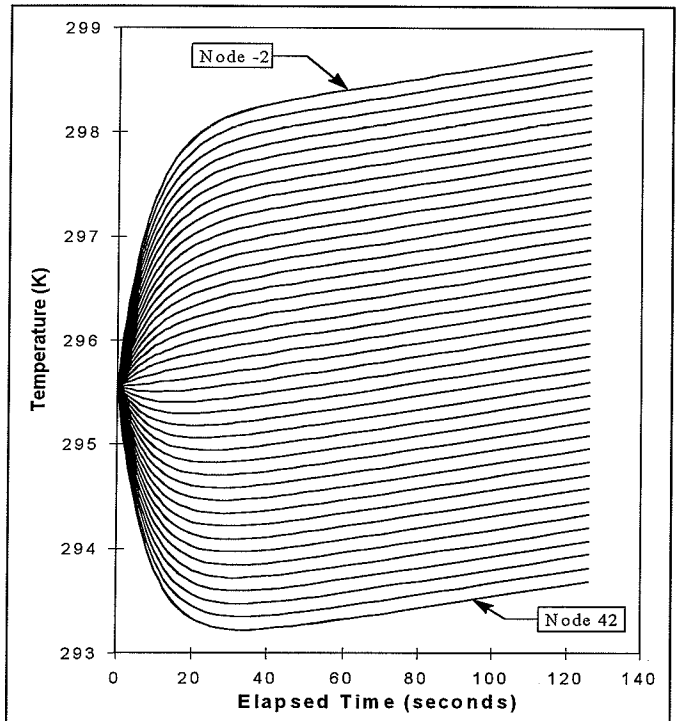

Fig. 7. Nodal Temperatures for Suspended Module. Power on. (Current = 0.0885 A)

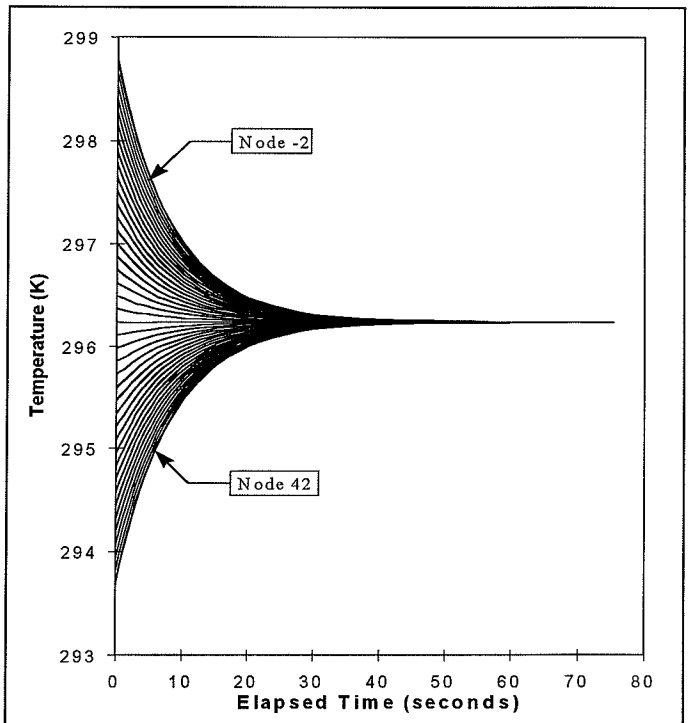

Fig. 9. Nodal Temperatures for suspended Module. Power off. (Initially at steady state, Current = 0 A)

Figure 10 displays the model results of the heat-sunk module temperature profiles at given time steps for the applied test current. Figure 11 shows how the nodal temperatures varied with respect to time. Figures 12 and 13 are similar to Figures 10 and 11 except are for the power-off condition.

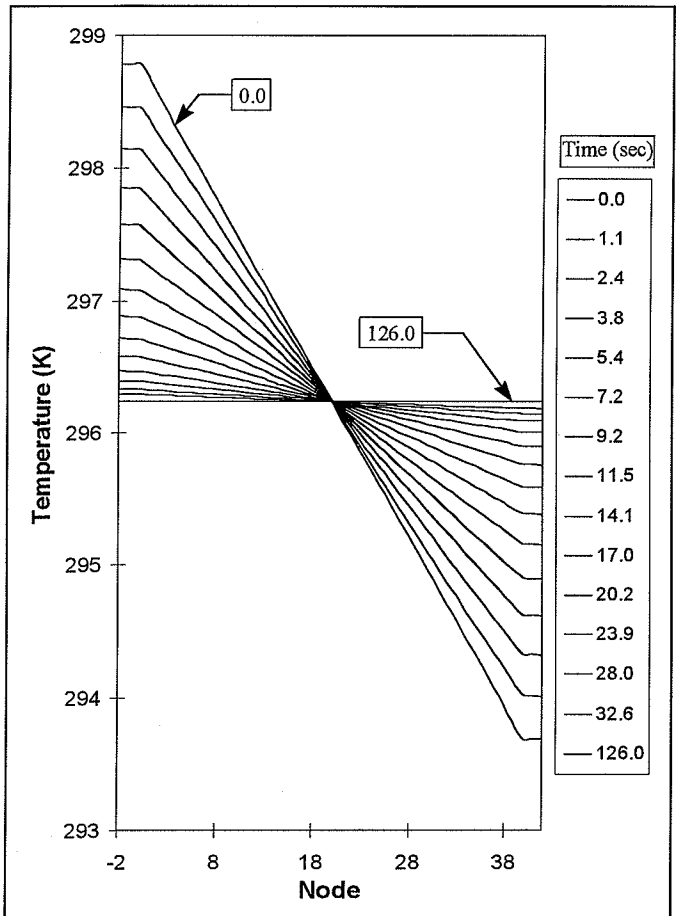

Fig. 8. Temperature Profile for Suspended Module. Power off. (Initially at steady state, Current = 0.0885 A)

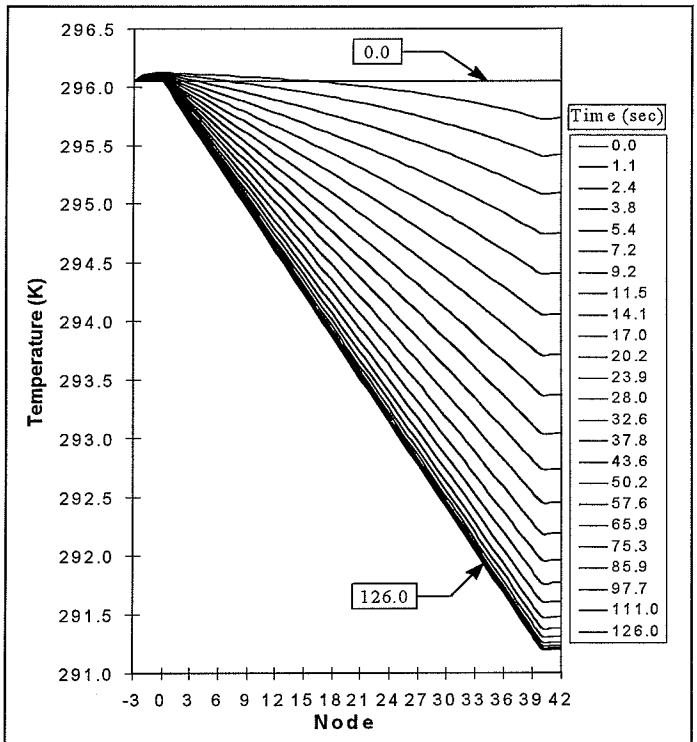

Fig. 10. Temperature Profiles for Heat Sunk Module. Power on. (Current = 0.0885 A)

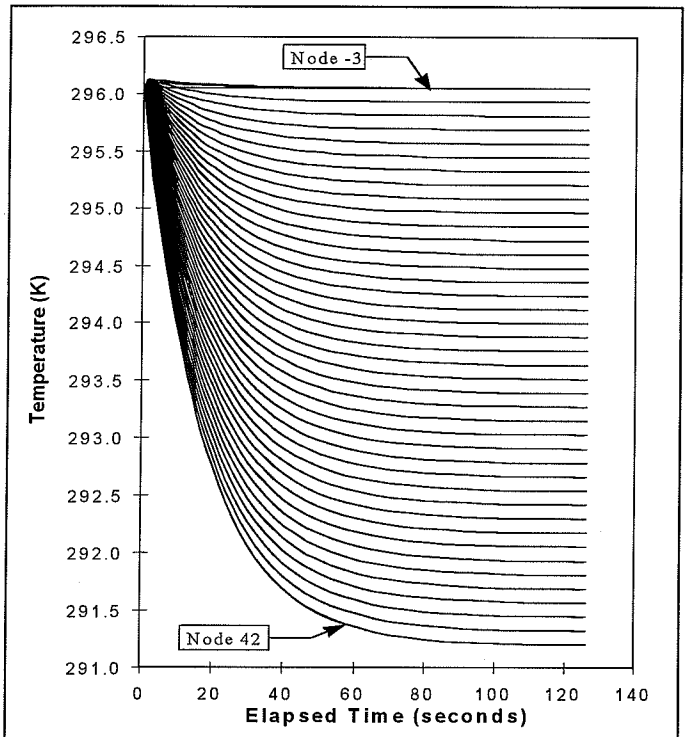

Fig. 11. Nodal Temperatures for Heat Sunk Module. Power on. (Current = 0.0885 A)

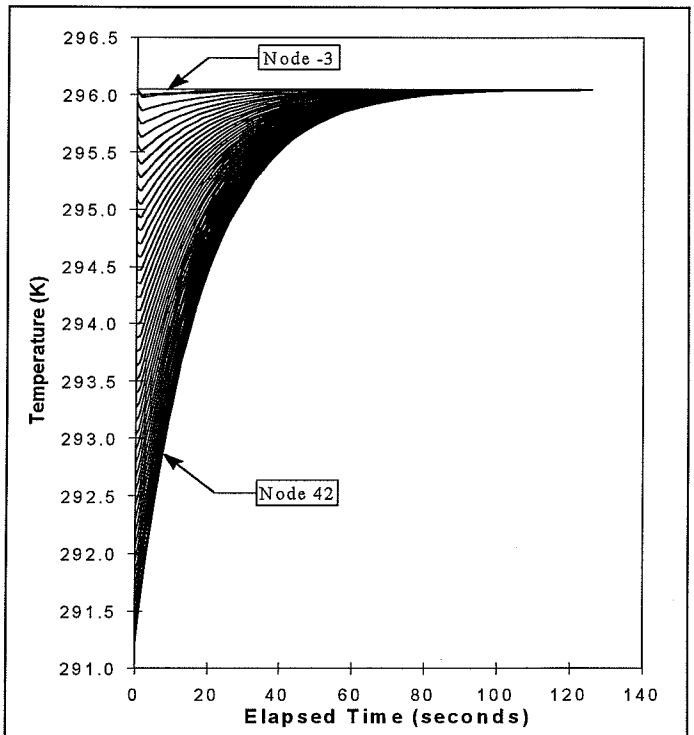

Fig. 13. Nodal Temperature for Heat Sunk Module. Power off. (Initially at steady state, Current = 0.0885 A)

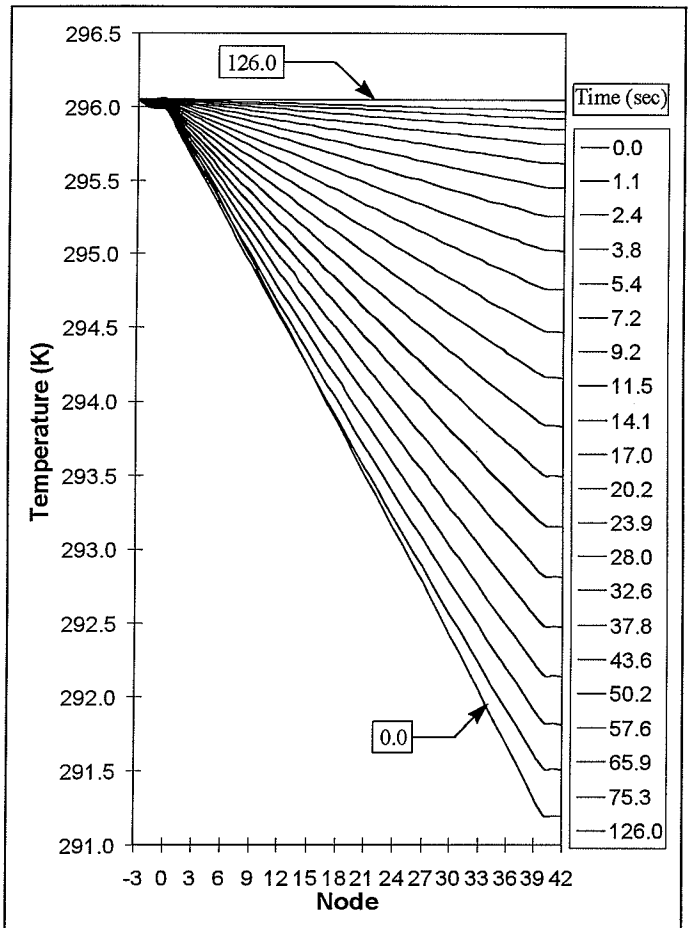

Fig. 12. Temperature Profiles for Heat Sunk Module. Power off. (Initially at steady state, Current = 0.0885A)

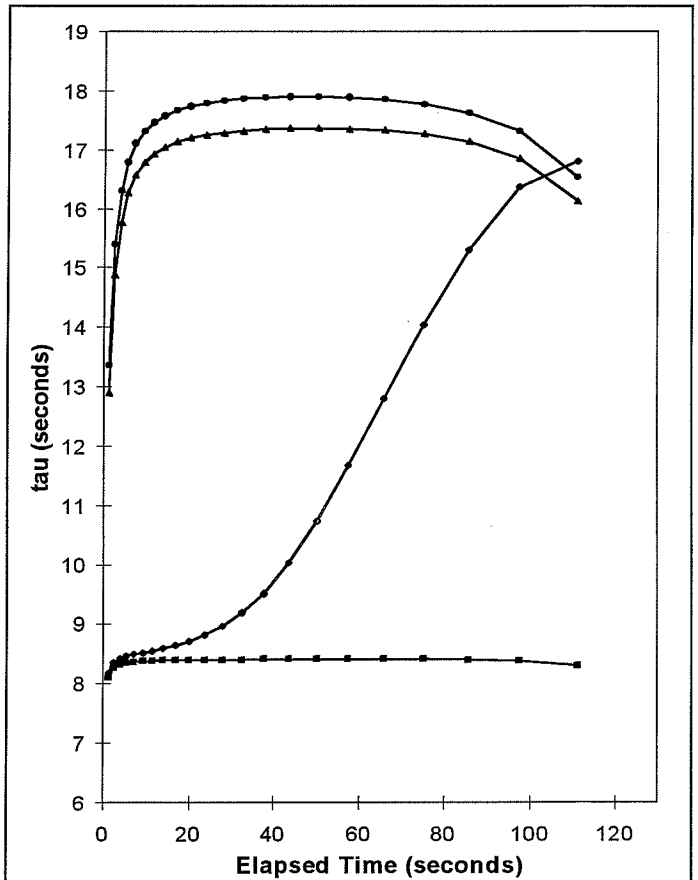

Fig. 14. Calculated Time Constants.

$$V = V_\infty + (V_0 - V_\infty)\exp\left(-t/\tau\right)$$

Figure 14 shows how the "time constant", tau, varied with respect to time. This time constant is based on the equation:

$$V = V_\infty + (V_0 - V_\infty)\exp\left(-t/\tau\right) \qquad (6)$$

which is normally applicable to resistance-capacitance electrical circuits. Of course, a time constant for a suspended module has no practical use. However, for the heat-sunk configuration, it was evident that a true time constant based on equation (6) did not exist.

Conclusions

The model correlated well with the test results. However, some refinements could be made to improve the model. The model used N and P-type averaged material properties. Therefore, some error was introduced by this averaging. Also, the actual TE pellet dimensions varied from one pellet to the next. The model used average pellet dimensions, so more error was introduced. Nonetheless, the finite-element model captures the fast, transient response of TE modules to an applied current.

This capability is especially important when the results presented in Figure 14 are considered. The use of a simple, time-constant analysis to characterize the transient response of a heat-sunk module would be inaccurate, especially in the first moments of applied current. However, the finite-element model is very accurate in the first moments of applied current.

References

[1] A. Bejan, *Advanced Engineering Thermodynamics*, John Wiley & Sons, Inc., New York (1988).

[2] R. J. Buist, "Calculation of Peltier Device Performance", *CRC Handbook of Thermoelectrics*, edited by D.M. Rowe, pp. 143-155 (1995).

[3] S.C. Chapra and R.P. Canale, *Numerical Methods for Engineers*, McGraw-Hill, Inc., New York (1988).

[4] F. Kiya, M. Sakai, T. Tanaka. Y. Ogawa, K. Mukasa, N. Sasa, and J. Nagao, "Computer Based Analysis of TE Cooling Device", in *Proceedings of the 12th International Conference of Thermoelectrics*, pp. 417-420 (1993).

[5] R.J. Buist, "A New Method for Testing Thermoelectric Materials and Devices", *11th International Conference on Thermoelectrics*, Arlington, Texas, USA, (1992).

[6] D.R. Lide, *CRC Handbook of Chemistry and Physics*, CRC Press, Florida (1992-1993).